

# Second Order Bounce Back Boundary Condition for the Lattice Boltzmann Fluid Simulation

In Chan Kim\*

(Kunsan National University)

A new bounce back boundary method of the second order in error is proposed for the lattice Boltzmann fluid simulation. This new method can be used for the arbitrarily irregular lattice geometry of a non-slip boundary. The traditional bounce back boundary condition for the lattice Boltzmann simulation is of the first order in error. Since the lattice Boltzmann method is the second order scheme by itself, a boundary technique of the second order has been desired to replace the first order bounce back method. This study shows that, contrary to the common belief that the bounce back boundary condition is unilaterally of the first order, the second order bounce back boundary condition can be realized. This study also shows that there exists a generalized bounce back technique that can be characterized by a single interpolation parameter. The second order bounce back method can be obtained by proper selection of this parameter in accordance with the detailed lattice geometry of the boundary. For an illustrative purpose, the transient Couette and the plane Poiseuille flows are solved by the lattice Boltzmann simulation with various boundary conditions. The results show that the generalized bounce back method yields the second order behavior in the error of the solution, provided that the interpolation parameter is properly selected. Coupled with its intuitive nature and the ease of implementation, the bounce back method can be as good as any second order boundary method.

**Key Words** : Lattice Boltzmann Method, Lattice BGK Method, Lattice Gas Approximation, Bounce Back Boundary Condition, Interpolation Parameter, Transient Couette Flow, Plane Poiseuille Flow

## 1. Introduction

Since Frisch *et al.* (1986) introduced the lattice gas automata (LGA) as an alternative numerical solver for the Navier-Stokes equation, the LGA experienced various changes and refinements to meet the ever increasing demands of the numerical science. The lattice Boltzmann method (LBM), introduced by McNamra & Zanetti (1988), is a successful offspring of the LGA. Unlike its predecessor, the LBM adopts real

numbers of the particle distribution and thus reduces the statistical noise inevitable in the use of the Boolean particle distribution of the LGA. After coming through a few modifications, the LBM was simplified into the lattice Bhatnagar-Gross-Krook (Bhatnagar *et al.*, 1954) or the LBGK model by Qian *et al.* (1992). Today, most LBM calculations adopt the LBGK model.

For the non-slip interface boundary between the fluid and the solid, the so-called bounce back boundary condition has traditionally been used. In the bounce back boundary condition, a particle arriving at the non-slip boundary bounces back to the incoming direction keeping its speed unchanged. It is widely believed that the bounce back boundary condition is of the first order in error. Being of the first order in error implies that the numerical error of the LBM solution from the

\* Corresponding Author,

E-mail : ickim@knusun1.kunsan.ac.kr

TEL : +82-654-469-4720 ; FAX : +82-654-469-4727  
School of Mechanical Engineering Kunsan National University, Miryong-dong 68, Kunsan, Chonbuk 573-701, Korea. (Manuscript Received March 12, 1999 ; Revised October 11, 1999)

exact solution reduces linearly with the mesh size. Since the lattice Boltzmann equation itself is of the second order, second order techniques have been desired to replace the first order bounce back boundary condition. A few of such methods has been recently devised (Noble *et al.*, 1995; Inamuro *et al.*, 1995; Maier *et al.* 1996; Chen *et al.*, 1996) reflecting its inventor's own insight and reasoning.

In this paper, the bounce back boundary condition is reconsidered. With the development of other second order techniques, the bounce back technique appears to be obsolete except for the educational purpose. We show, however, that contrary to the common belief that the bounce back boundary condition is unilaterally of the first order, there exists a class of bounce back boundary techniques that can be characterized by a single interpolation parameter. By using a properly chosen interpolation parameter in accordance with the detailed lattice geometry of the boundary, one can realize the second order boundary condition. Illustrative calculations are carried out for the transient Couette and the plane Poiseuille flows on the two dimensional square lattices. The calculation results for both test flows confirm that the bounce back boundary conditions yield the second order behavior in error when used with proper interpolation parameters.

## 2. Lattice Boltzmann Method

Consider a fluid particle moving in the two dimensional square lattices (d2q9 in Qian *et al.*, 1992), of which a unit cell is drawn in Fig. 1. Here, each lattice is connected to its neighbors by direction vectors

$$\mathbf{e}_i = \begin{cases} (0, 0), & i=0, \\ (\cos\frac{(i-1)\pi}{2}, \sin\frac{(i-1)\pi}{2}), & i=1, 2, 3, 4, \\ (\cos\frac{(2i-9)\pi}{4}, \sin\frac{(2i-9)\pi}{4}), & i=5, 6, 7, 8. \end{cases} \quad (1)$$

In the lattice Boltzmann fluid simulation, the primary variable is the particle distribution  $f_i(\mathbf{x}, t)$  defined as the fractional number of fluid particles at a position  $\mathbf{x}$  and time  $t$  moving in the direction of  $\mathbf{e}_i$ . Mass and momentum are related to  $f_i$  by

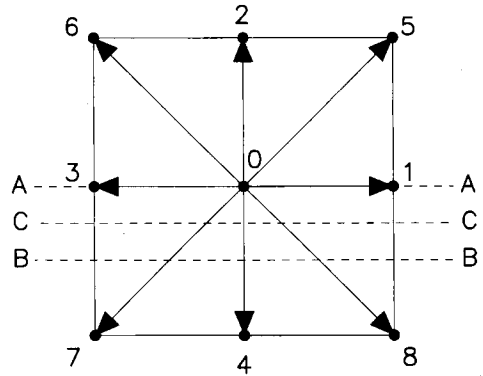


**Fig. 1** Unit cell for a particle in the two dimensional square lattices. In the figure, the line A includes the lattice sites 3, 0, 1. The line B lies halfway between the line A and the line connecting the lattice sites 7 and 8. The line C lies halfway between the lines A and B

$$\rho = \sum_{i=0}^8 f_i, \quad (2)$$

and

$$\rho \mathbf{u} = \sum_{i=0}^8 f_i \mathbf{e}_i, \quad (3)$$

where  $\rho$  and  $\mathbf{u}$  denote the density and the velocity, respectively. The time evolution of  $f_i$  is computed by (Chen *et al.*, 1992)

$$f_i(\mathbf{x} + \mathbf{e}_i, t+1) = f_i(\mathbf{x}, t) + \mathcal{Q}_i[f(\mathbf{x}, t)], \quad (4)$$

which implies that  $f_i$  at the new time consists of two distinct contributions: the streaming part  $f_i(\mathbf{x}, t)$  and the collision part  $\mathcal{Q}_i$ . The streaming term represents the advection of the particle and the collision term represents the local change in the particle distribution due to the particle collision. In the Bhatnagar–Gross–Krook approximation (Bhatnagar *et al.*, 1954), the collision operator  $\mathcal{Q}_i$  is expressed in the simple linear form with single relaxation time  $\tau$  toward the equilibrium

$$\mathcal{Q}_i(f) = -\frac{1}{\tau}(f_i - f_i^{eq}), \quad (5)$$

resulting in the LBGK equation

$$f_i(\mathbf{x} + \mathbf{e}_i, t+1) = f_i(\mathbf{x}, t) - \frac{1}{\tau}(f_i(\mathbf{x}, t) - f_i^{eq}(\mathbf{x}, t)), \quad (6)$$

where  $f_i^{eq}$  is the equilibrium distribution. For square lattices,  $f_i^{eq}$  can be chosen in the following form (Qian *et al.*, 1992):

$$f_0^{eq} = \frac{4}{9} \left[ 1 - \frac{3}{2} (\mathbf{u} \cdot \mathbf{u}) \right], \quad (7)$$

$$f_i^{eq} = \frac{1}{9} \left[ 1 + 3(\mathbf{e}_i \cdot \mathbf{u}) + \frac{9}{2} (\mathbf{e}_i \cdot \mathbf{u})^2 - \frac{3}{2} (\mathbf{u} \cdot \mathbf{u}) \right],$$

$$i = 1, 2, 3, 4, \quad (8)$$

$$f_i^{eq} = \frac{1}{36} \left[ 1 + 3(\mathbf{e}_i \cdot \mathbf{u}) + \frac{9}{2} (\mathbf{e}_i \cdot \mathbf{u})^2 - \frac{3}{2} (\mathbf{u} \cdot \mathbf{u}) \right],$$

$$i = 5, 6, 7, 8. \quad (9)$$

The Navier-Stokes equations are recovered by performing a Taylor expansion of the LBGK Eq. (6) in time and space using a Chapman-Enskog procedure. The LBGK Eq. (6) with appropriate initial and boundary conditions completes the lattice Boltzmann algorithm. We only need to consider the boundary conditions.

### 3. Boundary Condition

Since its introduction in the earlier form of the lattice gas approximation, the lattice Boltzmann method has traditionally been used with the bounce back boundary condition for the particles at the non-slip interface boundary. In the bounce back method, particles moving toward the solid wall reflect back into the opposite direction in the fluid region, keeping their speeds unchanged. Consider, for example, the particles at the bottom boundary. From here and on, boundary conditions are considered for the representative case of the bottom boundary. However, arguments given below can be also applied for non-slip boundaries other than the bottom one. Let us denote a unit cell at the bottom boundary in Fig. 1. Let us first assume that the fluid-solid interface boundary is at the line A. Then, the lattice sites 6, 2, 5 above the boundary belong to the fluid and the lattice sites 7, 4, 8 below the boundary belong to the solid. The lattice sites 3, 0, 1 are right on the boundary. At the time  $t$ , the particles are at the node 0 of which the position is  $\mathbf{x}$ . The particles at  $(\mathbf{x}, t)$  moving in the directions of  $\mathbf{e}_4, \mathbf{e}_7, \mathbf{e}_8$  into the solid region reflect back into the position  $\mathbf{x}$ , turning to the opposite directions  $\mathbf{e}_2, \mathbf{e}_5, \mathbf{e}_6$ , respectively, at the next time  $t+1$ . This can be explicitly written as, for the particle distributions  $f_2, f_5, f_6$ ,

$$f_2(\mathbf{x}, t+1) = f_4(\mathbf{x}, t) - \frac{1}{\tau} [f_4(\mathbf{x}, t) - f_4^{eq}(\mathbf{x}, t)], \quad (10)$$

$$f_5(\mathbf{x}, t+1) = f_7(\mathbf{x}, t) - \frac{1}{\tau} [f_7(\mathbf{x}, t) - f_7^{eq}(\mathbf{x}, t)], \quad (11)$$

$$f_6(\mathbf{x}, t+1) = f_8(\mathbf{x}, t) - \frac{1}{\tau} [f_8(\mathbf{x}, t) - f_8^{eq}(\mathbf{x}, t)], \quad (12)$$

The particles at  $(\mathbf{x}, t)$  moving in the directions other than  $\mathbf{e}_4, \mathbf{e}_7, \mathbf{e}_8$  stream and collide by the LBGK Eq. (6):

$$f_0(\mathbf{x}, t+1) = f_0(\mathbf{x}, t) - \frac{1}{\tau} [f_0(\mathbf{x}, t) - f_0^{eq}(\mathbf{x}, t)], \quad (13)$$

$$f_1(\mathbf{x} + \mathbf{e}_1, t+1) = f_1(\mathbf{x}, t) - \frac{1}{\tau} [f_1(\mathbf{x}, t) - f_1^{eq}(\mathbf{x}, t)], \quad (14)$$

$$f_2(\mathbf{x} + \mathbf{e}_2, t+1) = f_2(\mathbf{x}, t) - \frac{1}{\tau} [f_2(\mathbf{x}, t) - f_2^{eq}(\mathbf{x}, t)], \quad (15)$$

$$f_3(\mathbf{x} + \mathbf{e}_3, t+1) = f_3(\mathbf{x}, t) - \frac{1}{\tau} [f_3(\mathbf{x}, t) - f_3^{eq}(\mathbf{x}, t)], \quad (16)$$

$$f_5(\mathbf{x} + \mathbf{e}_5, t+1) = f_5(\mathbf{x}, t) - \frac{1}{\tau} [f_5(\mathbf{x}, t) - f_5^{eq}(\mathbf{x}, t)], \quad (17)$$

$$f_6(\mathbf{x} + \mathbf{e}_6, t+1) = f_6(\mathbf{x}, t) - \frac{1}{\tau} [f_6(\mathbf{x}, t) - f_6^{eq}(\mathbf{x}, t)], \quad (18)$$

The bounce back method that used Eqs. (10)–(18) has traditionally been used in conjunction with the boundary at the regular lattice sites, as denoted by the line A in Fig. 1. This bounce back method is known as being of the first order in error, implying that the numerical error of the LBGK solution from the exact solution reduces linearly with the mesh size. We refer to this boundary method as the traditional bounce back or TBB method.

A variant of the TBB method is the one obtained by locating the boundary off the regular lattice sites, halfway between the nodes. Let us denote this boundary by the line B in Fig. 1. In this boundary condition, the lattice sites 3, 0, 1 as well as the lattice sites 6, 2, 5 belong to the fluid and the lattice sites 7, 4, 8 belong to the solid. The bounce back method that uses Eqs. (10)–(18) in conjunction with the boundary off the regular lattice sites, as denoted by the line B, has been frequently referred to as the shifted bounce back or SBB method, since the boundary is shifted from the regular lattice sites. The SBB method is known to have better error characteristics than the TBB method. Indeed, the SBB method is found to be of the second order in error while the TBB method is of the first order. (Chen *et al.*, 1996) Why is it so? An answer lies at the observation that the right hand side of Eq. (10), for

example, is equal to  $f_4(\mathbf{x} + \mathbf{e}_4, t+1)$  by the LBGK Eq. (6). A particle moving in the direction of  $\mathbf{e}_4$  at  $(\mathbf{x}, t)$  at the node 0 first tries to move into the position  $\mathbf{x} + \mathbf{e}_4$  at the node 4 in the solid region at the new time  $t+1$ . Since the position  $\mathbf{x} + \mathbf{e}_4$  is not allowed for the fluid particle, the particle takes the alternative position  $\mathbf{x}$  instead of  $\mathbf{x} + \mathbf{e}_4$  at the time  $t+1$ . This implies that the particle moving at the constant speed in the interval from  $(\mathbf{x}, t)$  to  $(\mathbf{x} + \mathbf{e}_4, t+1)$  experiences the specular reflection at  $(\mathbf{x} + \frac{1}{2}\mathbf{e}_4, t + \frac{1}{2})$ . Thus, the particle bouncing back by Eq. (10) *feels* as if the boundary is located at the line B in Fig. 1, halfway between the node 0 and the node 4. Similarly, the particles bouncing back by Eqs. (11), (12) feel as if the boundary is located halfway between the nodes 3, 1 and the nodes 7, 8. This suggests that the bounce back of the particles is better accounted for by the SBB method than by the TBB method and explains why the SBB method yields the better error characteristics.

The specular reflection exactly at the regular lattice sites, as denoted by the line A in Fig. 1, can be realized by letting it take place for a unit time interval from  $t$  to  $t+1$ , instead of the instant reflection at  $t + \frac{1}{2}$ . A particle, for example, moving in the direction of  $\mathbf{e}_4$  finds that the destination is not allowed and then spends a unit time to turn to the opposite direction into the fluid, keeping its speed unchanged. For the particles moving in the directions of  $\mathbf{e}_4, \mathbf{e}_7, \mathbf{e}_8$  into the solid at  $(\mathbf{x}, t)$  at the node 0 in the bottom boundary, the particle distributions at the new time  $t+1$  can be simply written as

$$f_2(\mathbf{x}, t+1) = f_4(\mathbf{x}, t), \quad (19)$$

$$f_5(\mathbf{x}, t+1) = f_7(\mathbf{x}, t), \quad (20)$$

$$f_6(\mathbf{x}, t+1) = f_8(\mathbf{x}, t). \quad (21)$$

For the particles at  $(\mathbf{x}, t)$  moving in the directions other than  $\mathbf{e}_4, \mathbf{e}_7, \mathbf{e}_8$  into the fluid, the particle distributions at the new time  $t+1$  are given by Eqs. (13)–(18) as before. Calculations for the test problems, as given below in Section 4, show that the LBGK solution with the bounce back method of (19)–(21) and (13)–(18) in

conjunction with the boundary at the regular lattice sites, as denoted by the line A in Fig. 1, exhibits the second order behavior in error. Let us refer to this boundary method as the alternative bounce back boundary method or ABB method.

With the ABB method of the delayed reflection (19)–(21) at hand, the bounce back method can be generalized. This generalized bounce back method can be used for boundaries that lie at the arbitrary locations between the neighboring regular lattice sites. This generalization is done by linearly combining the above two different boundary methods, namely, the SBB and ABB methods. For the bottom boundary, if an interpolation parameter  $\omega$  is used for the particles moving in the directions of  $\mathbf{e}_4, \mathbf{e}_7, \mathbf{e}_8$ , the particle distributions  $f_2(\mathbf{x}, t+1), f_5(\mathbf{x}, t+1), f_6(\mathbf{x}, t+1)$  are then computed by

$$\begin{aligned} f_2(\mathbf{x}, t+1) &= (1-\omega)f_4(\mathbf{x}, t) + \omega \left\{ f_4(\mathbf{x}, t) - \frac{1}{\tau} [f_4(\mathbf{x}, t) \right. \\ &\quad \left. - f_4^{eq}(\mathbf{x}, t)] \right\} \\ &= f_4(\mathbf{x}, t) - \frac{\omega}{\tau} [f_4(\mathbf{x}, t) - f_4^{eq}(\mathbf{x}, t)], \quad (22) \end{aligned}$$

$$f_5(\mathbf{x}, t+1) = f_7(\mathbf{x}, t) - \frac{\omega}{\tau} [f_7(\mathbf{x}, t) - f_7^{eq}(\mathbf{x}, t)], \quad (23)$$

$$f_6(\mathbf{x}, t+1) = f_8(\mathbf{x}, t) - \frac{\omega}{\tau} [f_8(\mathbf{x}, t) - f_8^{eq}(\mathbf{x}, t)], \quad (24)$$

with any choice of  $0 \leq \omega \leq 1$ , where  $\omega/2$  is the ratio of the spacing between the boundary and the nearest fluid site to the mesh size. Letting  $\omega=0$  will make the reflection take place at the position  $\mathbf{x}$  of the line A in Fig. 1 and  $\omega=1$  at the position  $\mathbf{x} + \frac{1}{2}\mathbf{e}_4$  of the line B. Letting  $0 < \omega < 1$  will make the reflection take place in between. For example, letting  $\omega=1/2$  will make the reflection take place at the position  $\mathbf{x} + \frac{1}{4}\mathbf{e}_4$  on the boundary denoted by the line C in Fig. 1. In the figure, the line C is located off the regular lattice sites by the distance of the one fourth of the mesh size. In this generalized bounce back boundary condition with  $\omega=1/2$ , the lattice sites 3, 0, 1 as well as the lattice sites 6, 2, 5 belong to the fluid and the lattice sites 7, 4, 8 belong to the solid. Calculations for test problems, as given below in Section 4, show that the LBGK solution by the generalized bounce back

method of (22)–(24) and (13)–(18) with  $\omega=1/2$  in conjunction with the boundary at the line C in Fig. 1, exhibits the second order behavior in error. This confirms that the bounce back boundary technique can be satisfactorily used with the desired error characteristics of the LBGK method if it is properly used. By choosing a proper value for  $\omega$  in Eqs. (22)–(24) in accordance with the detailed lattice geometry of the boundary, one can obtain the bounce back boundary condition of the second order in error. The first order behavior of the traditional bounce back method was simply due to that its lattice geometry was not accordant with the bounce back boundary equations (10)–(18). Since the interpolation parameter  $\omega$  can be continuously varied in accordance with the local lattice geometry of the interface boundary, this generalized bounce back boundary method, unlike most other boundary methods, has the versatility to be easily used for any complex configuration of the boundary.

There exist other second-order boundary techniques that are different from the bounce back method. Noble *et al.* (1995) proposed a method in which the mass and the momentum are correctly conserved at the interface boundary. However, it is not clear if their method can be used other than two-dimensional hexagonal lattices. Maier *et al.* (1996) adjusted the particle distributions to achieve the non-slip velocity at the wall. Their method is equivalent to Noble's method, when used for two-dimensional hexagonal lattices. Inamuro *et al.* (1995) assumed the scattered reflection at the wall. They considered what they call the slip velocity and recalculated the equilibrium distribution with the counter slip velocity. They showed that the second order error characteristics were obtained by this for the transient Couette and the Poiseuille flows. Chen *et al.* (1996) introduced the additional nodes at the solid region and computed the particle distributions at these additional nodes. These extra nodes were used to obtain the unknown particle distributions at the interface boundary. In this study, simulation data for test flows are obtained by using the proposed bounce back boundary method as well as Inamuro's and Chen's methods.

#### 4. Test Results and Discussions

For the comparison of efficiencies of different bounce back methods, the LBGK simulations were carried out for test problems of the transient Couette and the plane Poiseuille flows. To estimate the numerical errors of different methods, the error  $E$  is defined as

$$E = \frac{\sum_{i=1}^N |\mathbf{u} - \mathbf{u}^*|^2}{\sum_{i=1}^N |\mathbf{u}^*|^2}, \quad (25)$$

where,  $\mathbf{u}$ ,  $\mathbf{u}^*$  are the LBGK and the exact solutions, respectively, and  $N$  is the number of lattice sites in the flow field.

In the transient Couette flow, the flow is driven by the shear motion of the top plate at  $y=L$ . At time  $t=0$ , the top plate starts to move in the positive  $x$  direction, at a constant speed  $U$ . The bottom plate at  $y=0$  remains at rest. The velocity distribution  $\mathbf{u}^*(\mathbf{x}, t)$  of the incompressible fluid of the kinematic viscosity  $\nu$  is given by, in the absence of external force field,

$$u^*(y, t) = U \left\{ \frac{y}{L} + \frac{2}{\pi} \sum_{n=1}^{\infty} \frac{(-1)^n}{n} \sin(n\pi y/L) \exp[-n^2\pi^2(\nu t)/L^2] \right\}, \quad (26)$$

$$v^*(y, t) = 0, \quad (27)$$

for  $0 \leq y \leq L$ , where  $u^*$ ,  $v^*$  are  $x$ ,  $y$  components of the velocity vector  $\mathbf{u}^*$ , respectively. Note that  $u^*(0, t) = 0$  and  $u^*(L, t) = U$  for  $t > 0$ . Figure 2 compares the LBGK solutions  $u$  for the transient Couette flow obtained by using the TBB boundary condition to the ones by the ABB boundary condition. Note that the ABB method is identical to the generalized bounce back method of (13)–(18), (22)–(24) with the interpolation parameter of  $\omega=0$ . For both LBGK calculations, the top and bottom boundaries were set to be located at the regular lattice sites as denoted by the line A in Fig. 1. The periodic boundary conditions were used for the left and right boundaries. Figure 2 also shows the exact solutions  $u^*$  for various values of the relaxation time  $\tau$ . In the figure, the LBGK solutions by the TBB and the new bounce back boundary methods are denoted by the filled triangles and circles, respectively. The solid lines

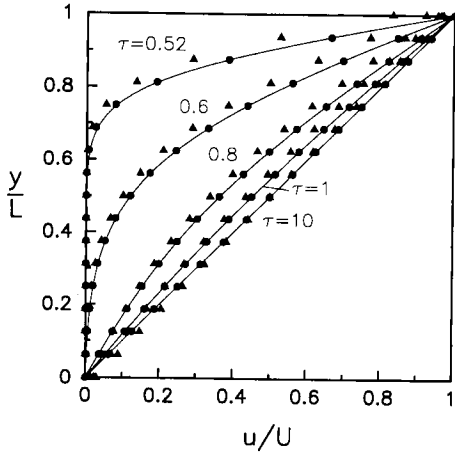


**Fig. 2** Velocity profiles of the transient Couette flow calculated by the LBGK method. The triangles and circles denote the LBGK results obtained by using the traditional and proposed bounce back methods, respectively. The solid lines represent the exact solutions for the respective values of  $\tau$ . Here,  $Re=10$ ,  $t=400$  and  $L=16$

denote the exact solutions  $u^*$  obtained by Eq. (26), for the respective values of  $\tau$ . Here, the number of nodes  $N$  in  $y$  direction was 17, the Reynolds number defined as  $Re=UL/\nu$  was set to be 10 and the time  $t$  was taken to be 400. The relaxation time  $\tau$ , that characterizes the relaxation speed toward the equilibrium, is related to the kinematic viscosity  $\nu$  by  $\nu=(2\tau-1)/6$  and thus required to be greater than 0.5. The error tends to be large for large  $\tau$ . It is because the Chapman-Enskog procedure breaks down for large  $\tau$ . For present calculation,  $\tau$  was taken to range from 0.52 to 10. It is seen in the figure that the errors of the LBGK solutions are much smaller when used with the ABB method than with the TBB method. This indicates that the LBGK method can have a better error characteristics if the boundary condition is properly used in accordance with the detailed lattice geometry of the boundary. The relative smallness of the LBGK errors were also observed in the LBGK calculations with the generalized bounce back boundary methods (13)-(18), (22)-(24) with other values of  $0 \leq \omega \leq 1$ , provided that they were accordant with the detailed lattice geometry of the boundary.

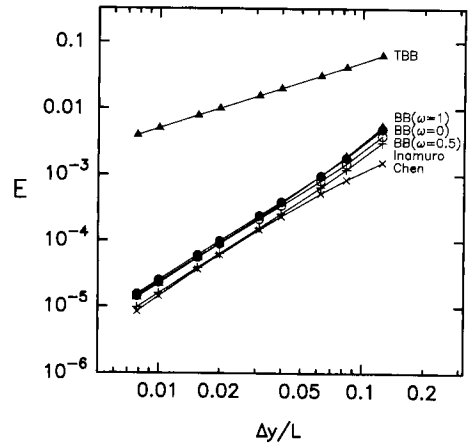


**Fig. 3** Measured errors of the LBGK solutions for the transient Couette flow. From top to bottom, the filled triangles, the hollow triangles, the filled circles, the hollow circles, '+' and 'x' signs denote the errors of the LBGK solutions obtained by the traditional bounce back method (TBB), the shifted bounce back method ( $BB(\omega=1)$ ), the generalized bounce back methods with  $\omega=0$  ( $BB(\omega=0)$ ) and  $\omega=0.5$  ( $BB(\omega=0.5)$ ), Inamuro's method (Inamuro) and Chen's method (Chen), respectively. Here,  $Re=10$ ,  $\tau=2$  and  $t/L^2=1$

In Fig. 3, the errors of the LBGK solutions for the transient Couette flow are summarized for various bounce back boundary conditions. Calculations were done for  $Re=10$ ,  $\tau=2$  and  $t/L^2=1$ . In the figure, the  $x$  and  $y$  axes denote the mesh size  $\Delta y/L$  and the numerical error  $E$ , respectively. The filled triangles and circles denote the LBGK errors for the TBB and ABB boundary conditions, respectively. The description 'BB( $\omega=0$ )' follows the filled circles, implying that it denotes the error of the LBGK solution using the generalized bounce back boundary condition (13)-(18), (22)-(24) with  $\omega=0$ . The slopes obtained by the least square fitting of the TBB and 'BB( $\omega=0$ )' data are estimated to be 1.00 and 2.05, respectively. This indicates that the generalized bounce back boundary method gives the LBGK solutions of the second order in error for the transient Couette flow, while the TBB boundary method gives the LBGK solutions of the first order. This result also confirms that the bounce

back method in accordance with the detailed lattice geometry of the boundary yields the better error characteristics. Note that for the generalized bounce back boundary method the lattice geometry is in accordance with the used boundary equations, while it is not for the TBB boundary method. The errors of the LBGK solutions obtained by using the SBB boundary method and the generalized bounce back method with  $\omega=0.5$  are also shown in Fig. 3. They are denoted by the hollow triangles and circles, respectively. The descriptions 'BB( $\omega=1$ )' and 'BB( $\omega=0.5$ )' follow the hollow triangles and circles, respectively. Note that the SBB boundary method is identical to the generalized bounce back method with  $\omega=1$ . For the LBGK simulation by using the SBB method, the top and bottom boundaries were set to be located halfway between the neighboring regular lattice sites, as denoted by the line B in Fig. 1. For the LBGK simulation by using the generalized bounce back method with  $\omega=0.5$ , the top and bottom boundaries were set to be displaced from the regular lattice sites by the one fourth of the mesh size, as denoted by the line C in Fig. 1. For all the simulations of the transient Couette flow, periodic boundary conditions were used for the left and right boundaries. The slopes obtained by the least square fitting of the 'BB( $\omega=1$ )' and the 'BB( $\omega=0.5$ )' data are estimated to be 2.12 and 1.95, respectively. This shows that the LBGK solutions with the generalized bounce back method gives the LBGK solutions of the second order in error for all values of  $\omega$ . Also included in the figure the LBGK results obtained by using other boundary techniques by Inamuro *et al.* (1995) and by Chen *et al.* (1996). For these calculations, the top and bottom boundaries were set to be located at the regular lattice sites, as denoted by the line A in Fig. 1. The errors by these methods are denoted by '+' and 'x' signs. The slopes obtained by the least square fitting of the data obtained by using Inamuro's and Chen's boundary methods are estimated to be 2.06 and 1.90, respectively. One could say that these boundary methods are also of the second order in error. In the figure, the errors of the data by the proposed bounce back method appear slightly

larger than the errors of the 'Inamuro' and 'Chen' data. However, considering that they are all second order scheme and the differences are rather small, it can't be definitely said that one method is better than the others. Moreover, the versatility of the proposed bounce back method to be suitable for use in the complex boundary configuration should make the proposed method as good as any second order scheme.

In the plane Poiseuille flow, the flow between the plates separated by the distance  $L$  is driven by the pressure gradient applied in the  $x$  direction. The top plate at  $y=L$  and the bottom plate at  $y=0$  remain at rest. The velocity distribution  $\mathbf{u}^*(\mathbf{x}, t)$  of the incompressible fluid is given by

$$u^*(y, t) = 4U \left( \frac{y}{L} - \frac{y^2}{L^2} \right), \quad (28)$$

$$v^*(y, t) = 0, \quad (29)$$

for  $0 \leq y \leq L$ , where the centerline velocity  $U$  is related to the pressure gradient  $dP/dx$  by  $U = -(dP/dx) (L^2/2\rho\nu)$ . The LBGK simulation for the plane Poiseuille flow were carried out by using various bounce back boundary conditions. Simulations were done for  $Re=10$  and  $\tau=2$ . For the LBGK simulation of the flow, the pressure gradient in the  $x$  direction was imposed by the following procedure: (i) The streaming and the collision were first calculated. (ii) Subsequently,  $f_1$  was increased by the amount of  $8\rho\nu U/3L^2$  and  $f_3$  was decreased by the same amount. (iii) Then,  $f_5, f_8$  were increased by the amount of  $2\rho\nu U/3L^2$  and  $f_6, f_7$  were decreased by the same amount. This procedure was applied for all the internal nodes as well as the ones at the top and bottom boundaries. For all the LBGK simulations for the plane Poiseuille flow, periodic boundary conditions were used for the left and the right boundaries. Errors of the obtained LBGK solutions are summarized in Fig. 4. In the figure, the  $x$  and  $y$  axes denote the mesh size  $\Delta y/L$  and the numerical error  $E$ , respectively. The layout of graphic symbols are same as in Fig. 3. In Fig. 4, the slope obtained by the least square fitting of the TBB (filled triangles) data is estimated to be 1.19. The 'BB( $\omega=0$ )' (filled circles), the 'BB( $\omega=0.5$ )' (hollow circles) and the 'BB( $\omega=1$ )' (hollow triangles) data are also shown in the figure. The

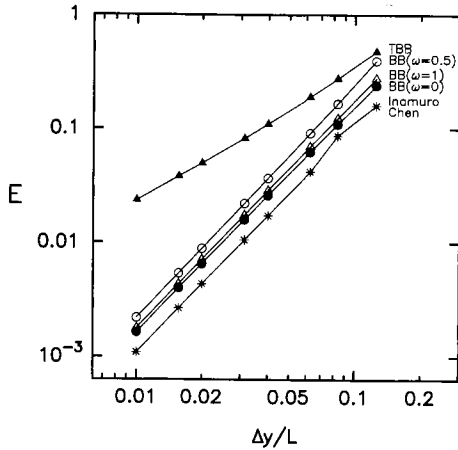


**Fig. 4** Measured errors of the LBGK solutions for the plane Poiseuille flow. From top to bottom, the filled triangles, the hollow circles, the hollow triangles, the filled circles, '+' and 'x' signs denote the errors of the LBGK solutions obtained by using the traditional bounce back (TBB) method, the generalized bounce back method with  $\omega=0.5$  [BB( $\omega=0.5$ )], the shifted bounce back method [BB( $\omega=1$ )], the generalized bounce back method with  $\omega=0$  [BB( $\omega=0$ )], Inamuro's method (Inamuro) and Chen's method (Chen), respectively. Here,  $Re=10$  and  $\tau=2$

slopes obtained by the least square fitting of these three data set are estimated to be 1.98 for BB( $\omega=0$ ), 2.06 for BB( $\omega=0.5$ ) and 2.00 for BB( $\omega=1$ ). This result indicates that the generalized bounce back boundary method gives the LBGK solutions of the second order in error for the plane Poiseuille flow, while the TBB boundary method gives the LBGK solution of the first order. Also included in the figure the errors of the LBGK solutions obtained by using the boundary conditions of Inamuro *et al.* (1995) and Chen *et al.* (1996). The slopes of these data, denoted by '+' and 'x' signs, are both estimated to be 2.00, implying that these methods are also of the second order. As in the transient Couette flow, the errors of the data by the proposed bounce back method appear slightly larger than the errors of the 'Inamuro' and 'Chen' data. However, they are all second order scheme and the differences are rather small. The versatility of the proposed bounce back method to be suitable for use in the

complex boundary configuration should make the proposed method as good as any second order scheme.

## 5. Conclusions

When used for the LBGK fluid simulation, the bounce back method, as traditionally used, yields the first order behavior in the error of the solution. On the contrary, its variant, the shifted bounce back method yields the second order behavior. The difference is that in the LBGK simulation by using the shifted bounce back method the detailed lattice geometry of the boundary is properly accounted for in accordance with the boundary equation, while it is not the case in the LBGK simulation by using the traditional bounce back method. A generalized bounce back method is proposed, in which the detailed lattice geometry is properly taken into account for any arbitrarily irregular lattice geometry of the boundary. This generalized bounce back method is realized by including a single interpolation parameter in the bounce back boundary equation that interpolates between two different second order bounce back methods. Using the proper value of this parameter in accordance with the detailed lattice geometry of the boundary results in the second order behavior in the error of the LBGK solution. For illustration of the efficiency of the new boundary method, test problems of the transient Couette and the plane Poiseuille flows have been solved by the LBGK method with various bounce back methods. The calculation results confirmed that the generalized bounce back boundary method yields the desired second order characteristics. The proposed bounce back boundary method is also noted for its versatility to be used for arbitrarily complex configuration of the interface boundary.

## Acknowledgements

The author gratefully acknowledges the support of the Korea Science Foundation under Grant No. 961-1008-068-2.



## References

- Bhatnagar P., Gross E. and Krook M., 1954, "A Model for Collision Processes in Gases. I. Small Amplitude Processes in Charged and Neutral One-Component Systems," *Physical Review*, Vol. 94, pp. 511~525.
- Chen H., Chen S. and Matthaeus W., 1992, "Recovery of the Navier-Stokes Equations Using a Lattice Gas Boltzmann Method," *Physical Review A*, Vol. 45, pp. R5339~R5342.
- Chen S., Martinez D. and Mei R., 1996, "On Boundary Conditions in Lattice Boltzmann Methods," *Physics of Fluids*, Vol. 8, pp. 2527~2536.
- Frisch U., Hasslacher B. and Pomeau Y., 1986, "Lattice-Gas Automata for the Navier-Stokes equation," *Physical Review Letters*, Vol. 56, pp. 1505~1512.
- Inamuro T., Yoshino M. and Ogino F., 1995, "A Non-slip Boundary Condition for Lattice Boltzmann Simulation," *Physics of Fluids*, Vol. 7, pp. 2928~2930.
- Maier R. S., Bernard R. S. and Grunau D. W., 1996, "Boundary Conditions for the Lattice Boltzmann Method," *Physics of Fluids*, Vol. 8, pp. 1788~1801.
- McNamara G. R. and Zanetti G., 1988, "Use of the Boltzmann Equation to Simulate Lattice-Gas Automata," *Physical Review Letters*, Vol. 61, pp. 2332~2335.
- Noble D. R., Chen S., Georgiadis J. and Buckius R. O., 1995, "A Consistent Hydrodynamic Boundary Condition for the Lattice Boltzmann Method," *Physics of Fluids*, Vol. 7, pp. 203~209.
- Qian Y. H., d'Humieres D. and Lallemand P., 1992, "Lattice BGK Models for Navier-Stokes Equation," *Europhysics Letters*, Vol. 17, pp. 479~484.